

Electrical and optical measurements on the first SCUBA-2 prototype 1280 pixel submillimeter superconducting bolometer array

Adam L. Woodcraft,^{a)} Peter A. R. Ade, Dan Bintley, Julian S. House, Cynthia L. Hunt, and Rashmi V. Sudiwala
Cardiff School of Physics and Astronomy, Cardiff University, Queen's Buildings, The Parade, Cardiff CF24 3AA, United Kingdom

William B. Doriese, William D. Duncan, Gene C. Hilton, Kent D. Irwin, Carl D. Reintsema, and Joel N. Ullom
Quantum Sensor Project, NIST, 325 Broadway, Boulder, Colorado 80305

Michael D. Audley,^{b)} Maureen A. Ellis, Wayne S. Holland, and Mike MacIntosh
United Kingdom Astronomy Technology Centre, Royal Observatory, Blackford Hill, Edinburgh EH9 3HJ, United Kingdom

Camelia C. Dunare, William Parkes, and Anthony J. Walton
Scottish Microelectronics Centre, The University of Edinburgh, The King's Buildings, Edinburgh EH9 3JF, United Kingdom

Jan B. Kycia
Department of Physics, University of Waterloo, 200 University Avenue West, Waterloo, Ontario N2L 3G1, Canada

Mark Halpern
Department of Physics and Astronomy, University of British Columbia, 6224 Agricultural Road, Vancouver, British Columbia V6T 1Z1, Canada

Eric Schulte
Raytheon Vision Systems, 75 Coromar Drive, Goleta, California 93117

(Received 12 July 2006; accepted 9 December 2006; published online 9 February 2007)

SCUBA-2 is a submillimeter camera being built for the James Clerk Maxwell Telescope in Hawaii. Bringing CCD style imaging to the submillimeter for the first time, with over 10 000 pixels, it will provide a revolutionary improvement in sensitivity and mapping speed. We present results of the first tests on a prototype 1280 pixel SCUBA-2 subarray; the full instrument will be made up of eight such subarrays. The array is made up of transition edge sensor (TES) detectors, with Mo/Cu bilayers as the sensing element. To keep the number of wires reasonable, a multiplexed readout is used. Unlike previous TES arrays, an in-focal plane multiplexer configuration is used, in which the multiplexing elements are located beneath each pixel. To achieve the required performance, the detectors are operated at a temperature of approximately 120 mK. We describe the results of a basic electrical and optical characterization of the array, demonstrating that it is fully operational. Noise measurements were made on several pixels and gave a noise equivalent power below 2.5×10^{-17} W Hz^{-0.5}, within the requirements for SCUBA-2. The construction of the testbed used to carry out these measurements is also described. © 2007 American Institute of Physics.

[DOI: [10.1063/1.2436839](https://doi.org/10.1063/1.2436839)]

I. INTRODUCTION

Astronomy at submillimeter wavelengths is a relatively new field. In the last decade, state of the art systems have improved from single pixel detectors to arrays of hundreds of pixels. There are huge advantages to be gained from increasing the number of pixels still further, if this can be done without compromising performance.

SCUBA-2 is an instrument which will provide these ad-

vantages. Operating at wavelengths of 450 and 850 μm , it is due to start operation on the James Clerk Maxwell Telescope on Mauna Kea, Hawaii, in 2006, replacing the highly successful 131 pixel SCUBA instrument.¹ SCUBA-2 will have over 10 000 pixels and will provide a revolutionary improvement in sensitivity and mapping speed compared with existing instruments.

These improvements require a substantially different design to previous submillimeter instruments. The instrument is considerably larger, containing a large cooled optical system as well as the detectors themselves. It requires cooling to lower temperatures than previous instruments, and has a complex thermal design in order to bring the different com-

^{a)}Present address: Royal Observatory, Edinburgh, Blackford Hill, Edinburgh EH9 3HJ, UK.

^{b)}Present address: Cavendish Laboratory, University of Cambridge, Madingley Road, Cambridge CB3 0HE, UK.

ponents to their required temperatures.^{2,3} However, the largest change is in the detectors. Bolometers are used as in previous instruments, since they are the most sensitive detectors for broadband measurements at submillimeter wavelengths.⁴ Most existing arrays use semiconductors as the temperature sensing element. However, these have reached the sensitivity limit possible for this technology. Moreover, it is difficult to scale these arrays to more than a few hundred pixels since they involve manual steps in the construction of the pixels and require separate wiring to each detector.

SCUBA-2 uses transition edge sensor (TES) detectors.⁵ These make use of the electrical properties of a superconductor. As the temperature of a superconductor is increased, it undergoes a phase transition into the normal (nonsuperconducting) state. While in this phase transition, which can be made to take place over a temperature range as small as a few millikelvins, the electrical resistance changes rapidly with temperature. This can result in a very sensitive detector. The detectors are operated with a constant voltage bias, providing negative feedback to temperature changes caused by changes in incident power. For example, an increase in temperature increases resistance and thus decreases Joule heating, causing the TES to cool. There is thus no need for active temperature control to ensure that it remains at the correct temperature for the superconducting transition.

In addition, this choice of detector permits an array to be fabricated with conventional micromachining techniques, and for a multiplexed readout to be used, reducing the wire count to a reasonable level.

One consequence of the high pixel count is that it is not practical to locate the multiplexer to one side of the detectors, as has been done before. To do so would increase the size of the instrument considerably and would also require an impractical number of wires between the detectors and the multiplexer. Instead, an in-focal-plane architecture is used, in which the multiplexing elements are located beneath each pixel. The detectors and multiplexer are fabricated on separate silicon wafers, with superconducting indium bump bonds carrying electrical signals between the two wafers for each pixel as well as providing mechanical bonding and thermal conduction. A similar design has been developed recently using silicon semiconductor detectors and a complementary metal-oxide semiconductor (CMOS) multiplexer. However, the noise properties do not meet the requirements of SCUBA-2.⁶

This article describes electrical and optical tests on the first prototype SCUBA-2 detector array. Previous tests for SCUBA-2 have been limited to measurements on single pixel detectors⁷ and multiplexers without detectors present.⁸ These tests are the first measurements on any detector array with an in-focal-plane multiplexer. The number of pixels is also substantially greater than for any previous TES array.

II. DESCRIPTION OF THE ARRAY

SCUBA-2 (Refs. 9 and 10) contains two detector arrays, one operating at wavelengths around $850\ \mu\text{m}$ and the other at $450\ \mu\text{m}$, with each array consisting of four subarrays.

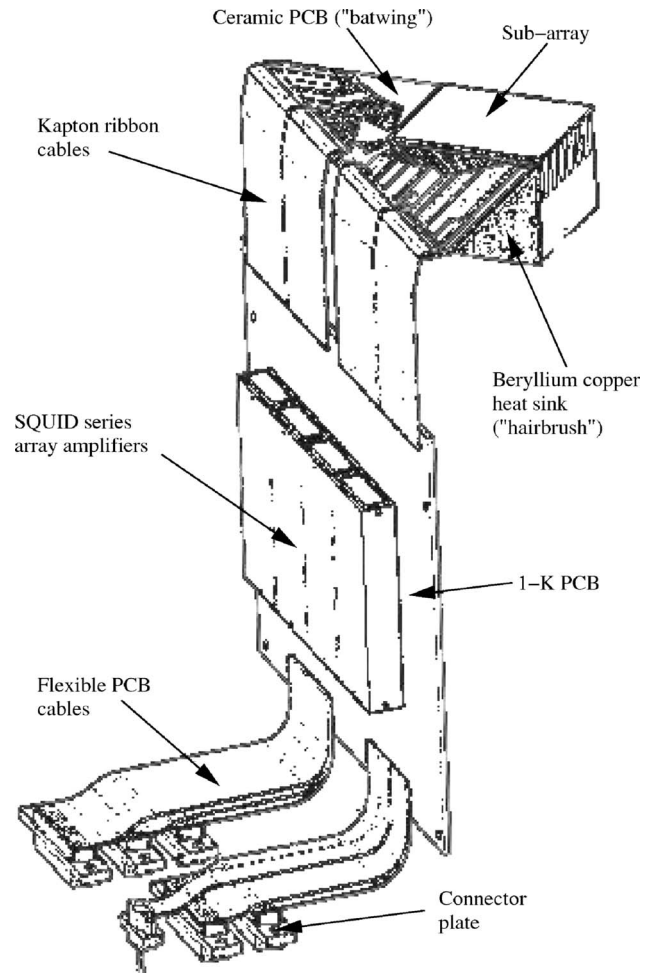


FIG. 1. The layout of a subarray unit.

Each subarray is contained within a subarray unit, which provides electrical and mechanical interfaces to the subarray, and also contains a circuit board maintained at a temperature of approximately 1 K. This article describes tests on a prototype $850\ \mu\text{m}$ subarray unit. A schematic is shown in Fig. 1. Detailed descriptions of the construction have already been given,^{9,10} therefore only a brief description will be provided here.

The subarray itself consists of a detector wafer and a multiplexer wafer. The detector wafer,^{11,12} fabricated from a 3 in. silicon wafer, contains the detectors themselves, arranged as 32 columns each with 40 rows. These consist of molybdenum-copper bilayer TES detectors, with the weak thermal link provided by a silicon nitride membrane. Each pixel is equipped with a resistive heater. This is used to compensate for changes in optical power as the sky background changes, enabling the pixels to be operated over a wide range of sky powers.⁷ The heaters are all wired in series. However, a high resistance shunt across each heater on the multiplexer wafer will ensure that the overall circuit is not broken if it is interrupted at any of the heaters.

The pixels are read out by a multiplexer^{8,13,14} fabricated on the silicon multiplexer wafer. Time division multiplexing is used; each pixel is connected to a superconducting quantum interference device¹⁵ (SQUID) via an input transformer⁸ and is addressed by biasing this SQUID. The output from

these SQUIDs is read out by a further SQUID for each column. The multiplexer wafer is bonded to the detector wafer using indium bump bonds; these carry electrical signals between the multiplexer and each pixel as well as bonding the two wafers together and providing thermal contact.¹¹ In addition to the SQUIDs under each pixel, the detector array contains a row of “dark” SQUIDs. These will be used to reduce $1/f$ noise, but were nonoperational for these tests due to a layout error in the multiplexer; this has been rectified in later multiplexers.

The subarray is glued to a beryllium-copper heat sink (the “hairbrush”).¹⁶ In operation, the hairbrush is cooled to a temperature of around 60 mK. It consists of a grid of independent tines, one underneath each pixel, providing mechanical support and thermal contact. The use of separate tines prevents stress from differential thermal contraction between the beryllium-copper and the silicon from damaging the wafers. To ensure that the tines are not bridged by a film of epoxy, a drop of epoxy is deposited independently on each tine prior to bonding using a commercial liquid deposition system.¹⁰

Wiring from the multiplexer is connected via wire bonds to a ceramic printed circuit board (PCB), called the “batwing,” also mounted on the hairbrush. Signals from this PCB are carried by ribbon cables to a further PCB maintained at a temperature of approximately 1 K. These cables consist of niobium tracks evaporated onto 50 μm thick Kapton® (type EN) ribbons, providing low thermal conduction. This is necessary since the heat leak from the 1 K stage to the detectors must be minimized. The 1 K PCB contains a SQUID series array amplifier¹⁷ for each column in the array. These consist of 100 SQUIDs in series, and convert the small signal output from the SQUIDs on the multiplexer to millivolt levels. Each pixel is thus read through three SQUID stages in series. The series array SQUIDs must be mounted on the 1 K PCB because the power dissipated is too great to be handled at millikelvin temperatures.

Flexible layers in the 1 K PCB extend to a connector plate. This provides a connection to the harness which runs to the room temperature electronics.

III. TESTBED

The measurements described here were carried out in the SCUBA-2 testbed, shown in Fig. 2. This is based around a custom-built cryostat¹⁸ which uses a dilution refrigerator for cooling to millikelvin temperatures.

The measurements described here were carried out with optical sources inside the cryostat. However, the cryostat is designed to permit direct external optical access to the array if required. This is achieved by having a shared vacuum space between the experimental area and the Dewar. The conventional arrangement for a dilution refrigerator is to have the dilution insert located in a “vacuum can” surrounded by liquid helium. To obtain optical access in this configuration would have required a helium-tight window at 4 K; this would be a potential reliability problem. Our arrangement has other advantages. A low temperature vacuum

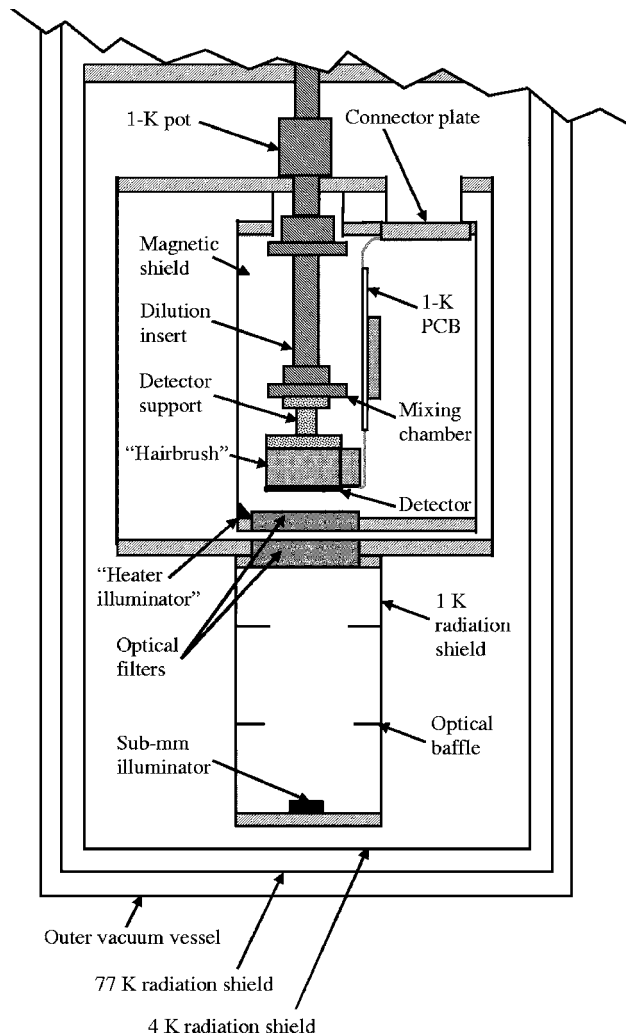


FIG. 2. The configuration of the testbed cryostat.

seal is not required, improving reliability, and the experimental space is maximized for a given cryostat diameter.

The main disadvantage is that exchange gas cannot be used to cool the system to 4 K; this is not a problem for these tests since we wished to avoid the use of exchange gas due to concerns over possible contamination of the detectors.

An acceptable cooldown time was achieved by using a mechanical heat switch linking the mixing chamber and 1 K pot of the dilution insert to the helium bath. Separate copper straps run from the mixing chamber and the 1 K pot to the heat switch. To close the switch, a worm drive operated from outside the cryostat is used to bring two copper blocks together, sandwiching a tongue at the end of each strap. To provide good thermal contact, all surfaces were gold plated. Using the heat switch gave a cooldown time of less than 2 days from room temperature to 77 K, and about a further 3 h to 4 K. The mass to be cooled consists mainly of approximately 18 kg of copper.

The testbed provides mechanical and electrical interfaces that match those in the actual SCUBA-2 instrument.^{3,16} This enables a subarray unit to be mounted in the testbed without modification. The 1 K PCB is cooled by the dilution refrigerator 1 K pot, and the detectors by the mixing chamber. In

addition to tests on prototype arrays, the testbed will be used to test each science grade array before integration with the instrument.

The array is located in a light-tight enclosure. Two sub-millimeter illuminators^{19,20} are mounted on the bottom of the enclosure. These consist of a resistive film deposited on a sapphire substrate. They have a time constant of approximately 0.2 s and can provide up to 3 fW of broadband illumination to each pixel.

Baffles in the optical path restrict reflections from the sides of the enclosure from reaching the detectors. Filters placed in front of the array and mounted on the 1 K structure control the wavelengths reaching the detectors from the illumination sources. A further illuminator (the “heater illuminator”) was mounted close to the array giving unfiltered access to the detectors; the location is shown in Fig. 2. This provides much greater power than the filtered illuminators and simulates the effects of sky power.

Magnetic shielding is provided to protect the SQUIDS from the effect of external magnetic shields. Layers of Metglas^{®21} (types 2705 and 2605SA1, unannealed) are used on the radiation shields at 77, 4, and 1 K. A further shield inside the main 1 K shield is covered with a layer of niobium foil over a layer of Metglas[®] 2705.

The wiring from room temperature to the subarray unit is identical to the harness to be used in the SCUBA-2 instrument. It consists of Monel clad niobium-titanium wires woven into a ribbon cable. The cables are heat sunk at temperatures of 4 and 2 K by clamping them between gold plated copper plates. Apiezon N grease is used to improve the thermal contact, and layers of cigarette paper prevent short circuits from the harness to the heat sink.

IV. RESULTS

A. operation

The readout system was capable of addressing a quarter of the subarray simultaneously. However, the parameters for the flux locked loop for each pixel have to be set up manually.^{13,14} This is a time consuming task, and therefore most measurements were carried out on a small number of pixels at a time. Future tests will be carried out with a prototype model of the electronics to be used at the telescope (known as the multichannel electronics or MCE). One such unit will be capable of addressing a full subarray, and ultimately will automatically select parameters for the flux locked loop, enabling straightforward simultaneous operation of each full subarray.

In total, 64 pixels were examined. Of these pixels, all were found to be fully functional at the level of the detector wafer. One pixel showed suboptimal performance on the multiplexer wafer, with a low current modulation depth¹³ preventing successful operation. The multiplexer was fully functional for the remaining pixels. Most measurements were made while multiplexing 8 or 16 pixels simultaneously. However, a set of 40 pixels was operated simultaneously, with no indication that there will be any difficulty multiplexing an entire subarray.

Due to the time consuming nature of making measurements on a large number of pixels with the present readout system, it was not possible to carry out every measurement on all of the 64 chosen pixels. Instead, a set of eight adjacent pixels in one column was chosen for more extensive examination, such as the load curve measurements described below. The choice of pixels was essentially random, although the column containing the one bad pixel described above was avoided.

Operation of the multiplexer was stable and reproducible from day to day. However, measurements on single pixels showed that the power dissipated in the first stage SQUID bias resistors could cause significant local heating and could even send the pixel into the normal state. This occurs because the conduction from the multiplexer wafer to the hairbrush is large compared with that laterally through the silicon, and heating is thus confined to a small area of the multiplexer. The thermal conduction from this small area through the glue to the heat sink is too low to provide sufficient cooling to the multiplexer wafer. Tests have shown that this will not be a problem in normal operation since multiplexing ensures that power is not applied to a given SQUID long enough for the local heating to be a problem.

There are also instabilities in the operation of the detectors at the lower resistance part of the superconducting transition. This can be explained by a model of the interaction between the flux from the input transformer and the portion of the TES directly over the transformer. As the current increases, the flux applied to that portion of the TES increases, increasing its resistance, which in turn causes the current to go down. Low in the transition, this negative feedback mechanism can lead to instability and oscillation. High in the transition, the portion of the TES over the transformer is driven fully normal by the flux, and the response should be stable. The pixels were always intended to be operated in the high resistance part of the transition. However, for robustness, this interaction will be broken in future arrays by replacing the portion of the TES directly over the flux transformer with low sheet resistance normal Cu film that is insensitive to the flux. Then operation should be stable throughout the superconducting transition. Despite these instabilities, it was possible to obtain an approximation to *I-V* measurements through the instability.

For these measurements, the heaters on the array were not available. The pixels are designed to operate with a significant fraction of the total power being applied from the heaters and/or optical background power. In the absence of the heaters, power from the heater illuminator was used. This is a valid method to make measurements; on the telescope the heater power is adjusted so that the total heating from absorbed sky power and the heaters is constant. In poor weather (high sky power), the heating will come mostly from absorbed optical power. However, this method causes photon shot noise that is higher than the noise that would be introduced by the heater. There is also a potential loss of uniformity due to the position of the source.

Since the detector bias and heater supplies for each pixel are wired in series, it is necessary for the array to be sufficiently uniform that all the pixels can be brought into an

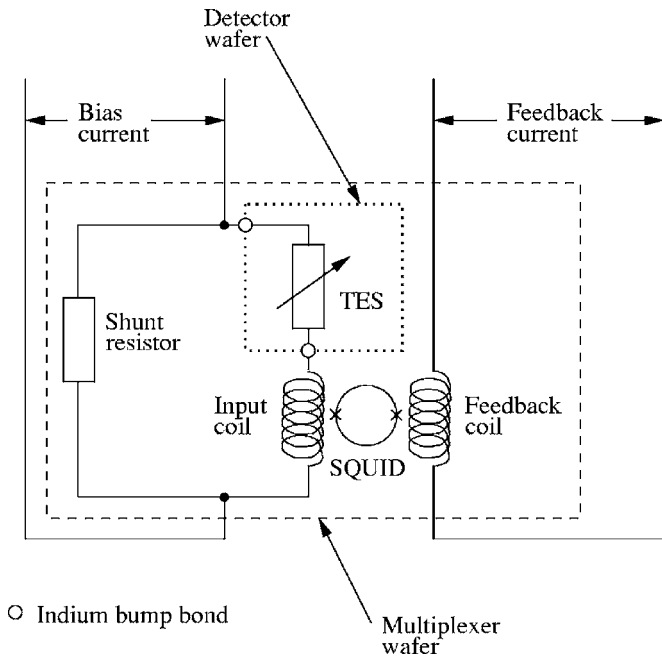


FIG. 3. The bias and feedback circuit for a single pixel. Each pixel also has a “dummy” SQUID, omitted from this diagram. These are never biased, but their presence reduces cross-talk.

operational state for the same bias and heater values. This requires the transition temperatures, conduction of the bolometer weak thermal links and from the multiplexer wafer to the hairbrush, and detector resistances to be similar across the array. While these properties have not been measured for every pixel, measurements at various points across the array indicate that all these properties are sufficiently uniform and that the entire array will be operable simultaneously.

B. Calibration

The current through each pixel is measured using a SQUID;¹⁵ the readout circuit for a single pixel is shown in Fig. 3. The output of a SQUID is periodic with respect to the sum of the magnetic flux from the input coils; the periodicity is given by a fundamental physical constant, the flux quantum. There is thus no unique output current for a given detector current. The SQUID is therefore used as a null detector, with current in the feedback coil being controlled by electronics to null out current through the detector coil which is in series with the TES. This feedback system is called a flux locked loop, and gives a linearized signal (the applied feedback current) which is proportional to the input current. Measurements using the flux locked loop are referred to here as closed loop measurements.

Calibration requires knowledge of the ratio of the mutual inductance between the SQUID and the two coils. This can easily be measured when the detector is in the superconducting state, since the resistance is zero, and thus the applied bias current passes entirely through the detector and the detector coil. The results of such measurements for 8 pixels are shown in Fig. 4. The measurements were made in closed loop mode by applying a modulated bias current to the detector and examining the resulting modulation in feedback current.

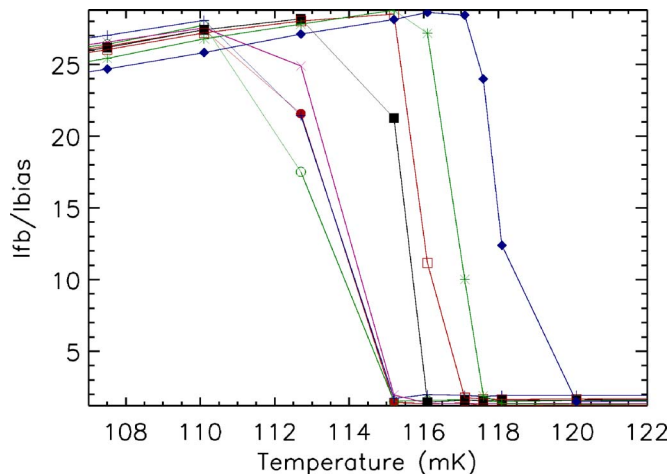


FIG. 4. (Color online) Measurements of the ratio of feedback current to bias current as a function of detector temperature, clearly showing the superconducting transition. The bias current was modulated with an amplitude of $7 \mu\text{A}$.

As the temperature is increased and the detectors pass from the superconducting state into the normal state, the current ratio falls by a large amount. This is because part of the bias current now passes through the shunt resistor, and the measured current through the detector decreases. The amount by which the ratio drops depends on the ratio of the shunt resistor and detector normal state resistance, and is in good agreement with the design values.

In the superconducting state, the current ratio falls slightly as the temperature is reduced. This is believed to be due to screening of the input coil by the TES.

The measurements in Fig. 4 show that the superconducting transition occurs over a narrow temperature range for each detector. The maximum variation between detectors is 5 mK and thus within the permissible range of 10 mK (chosen to allow simultaneous operation of all pixels in the array)

C. Load curves

Figure 5 shows measurements of the detector current as a function of bias current (“load curves”) for several pixels

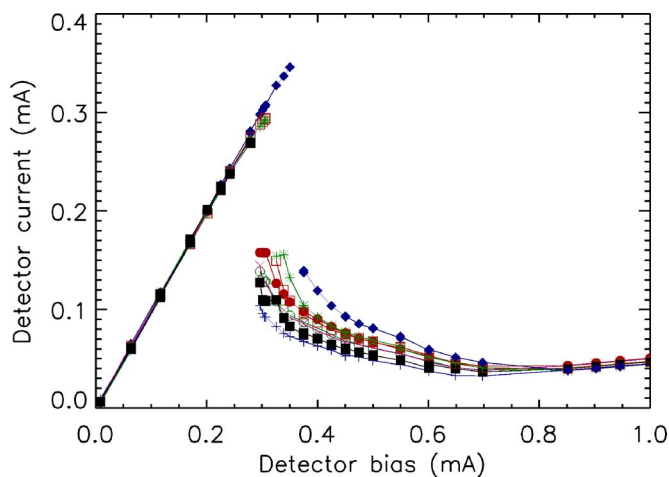


FIG. 5. (Color online) Detector current as a function of bias current (“load curves”) for 8 pixels measured simultaneously.

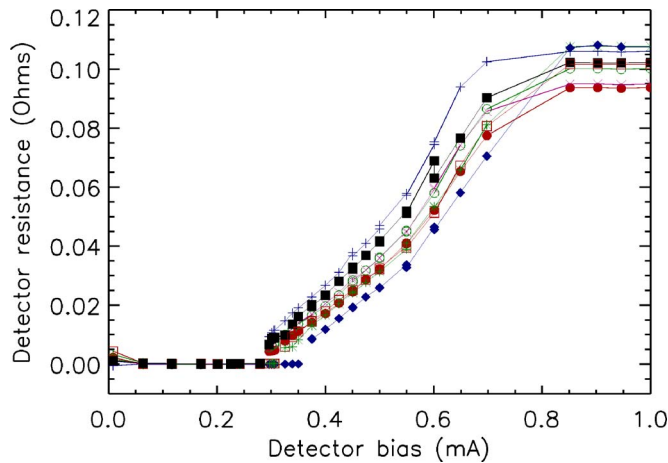


FIG. 6. (Color online) Detector resistance as a function of bias for 8 pixels measured simultaneously.

measured simultaneously. For these measurements the heat sink was maintained at a constant temperature of approximately 60 mK.

Since a SQUID only measures differential currents, it is necessary to remove an arbitrary offset from all the measurements. A load curve contains three distinct regions, in which the detector is either fully superconducting, in the superconducting transition, or fully normal. In the fully superconducting and fully normal state, the detector resistance should be constant to a very good approximation. The detector current should then be a linear function of the bias current with an intercept of zero, enabling the offset to be determined. This is not the case when the detector is in the superconducting transition; however, the offset determined from the fully normal state can be used. It is thus important to maintain continuity of measurements between the normal state and the transition region. At the low resistance end of the superconducting transition, the detector current varies very strongly with bias. It is thus not possible to make continuous measurements between the fully superconducting and transition regions, and there is a jump of an unknown number of flux quanta. The offset for the fully superconducting region thus has to be determined separately from that used in the transition and fully normal regions.

Figures 6 and 7 show the detector resistance and power, respectively. These values are obtained from the load curve shown in Fig. 5. However, in order to determine these values, it is necessary to know the voltage across the detector. This can be calculated from the current through the shunt resistor if its resistance is known. In the absence of an accurate method of measuring this, the design value of 5 m Ω was used. The true value is expected to be between 4 and 6 m Ω . Using either extreme value alters the absolute values in these figures; for example, the electrical power in the transition region increases or decreases by about 20%. However, the qualitative behavior is unchanged. In operation, the calibration will be based on optical measurements, not the assumed properties of the devices.

The resistance is constant in the superconducting and normal states, and the electrical power in the transition region is constant to a good approximation, as is expected for

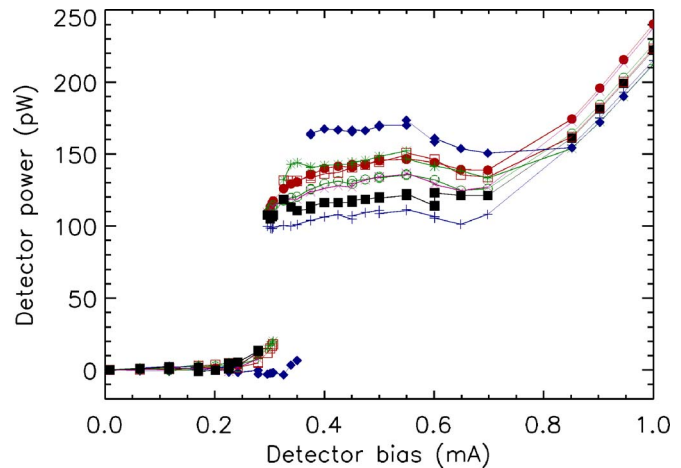


FIG. 7. (Color online) Detector electrical power as a function of bias for 8 pixels measured simultaneously.

TES devices.⁵ Note that the calibration method described above ensures that the detector resistance and power are zero in the superconducting region, so long as the resistance is constant.

The results of these measurements were repeatable from day to day, and were possible despite the instability of the detectors in the low part of the transition.

D. Optical response and NEP

Figure 8 shows the response from 2 pixels in multiplexed mode to a 2 Hz modulated optical power from the main illuminator.

Detector noise is a very important property of the arrays. We have measured the noise equivalent power²² (NEP) of several pixels by taking noise spectra while modulating the power from the submillimeter illuminator. For these measurements, the heater illuminator was used to keep the pixels in the superconducting transition for an appropriate range of bias levels; the location of the transition was determined by making load curve measurements as described above. Measurements were taken in the high bias part of the transition as is planned during normal operation.

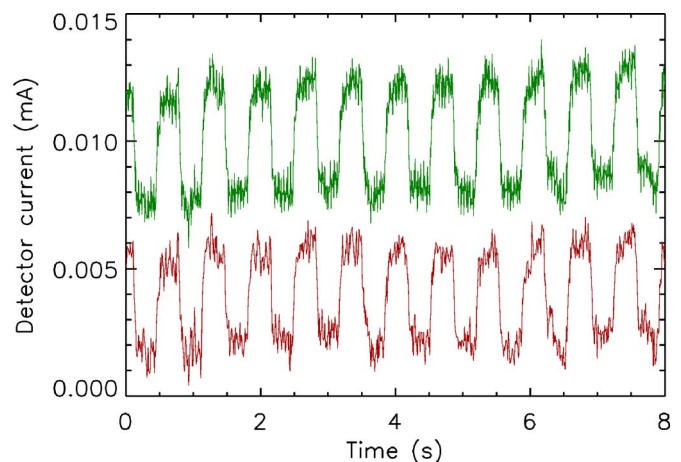


FIG. 8. (Color online) Response to modulated illumination (0.6 fW/pixel) for 2 pixels measured simultaneously. Each measurement has an arbitrary offset on the y axis.

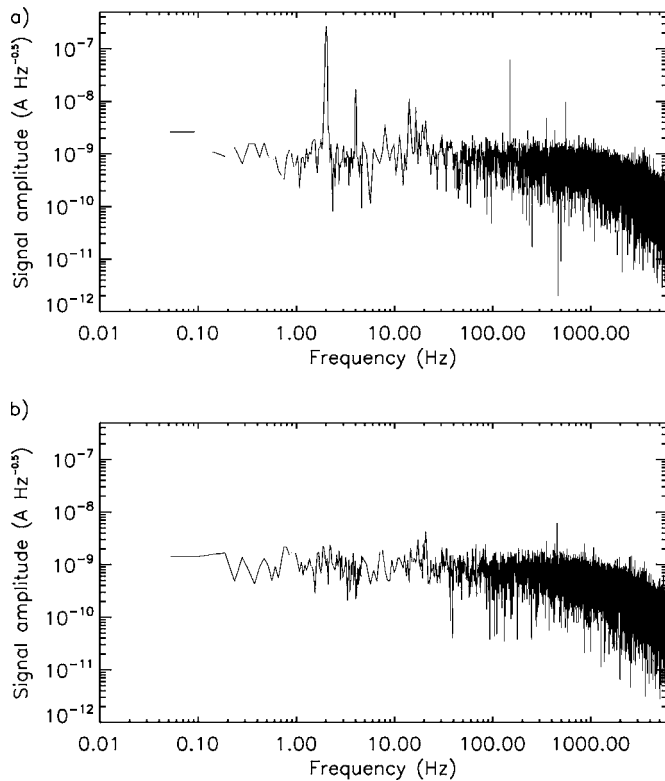


FIG. 9. Noise amplitude spectra for a single TES pixel detecting (a) a 2 Hz illuminator signal and (b) no signal. The noise values are similar for the two graphs, but graph (a) also shows a peak at a frequency of 2 Hz corresponding to the modulated signal from the illuminator. Similar results were obtained from the other pixels examined.

It is important to appreciate that the measured output signal is the real-time feedback current which is sampled (in closed loop mode) at a frequency of 48.8 kHz. This can be converted to the actual detector current using the calibration described in Sec. IV B. However, to estimate the NEP it is not necessary to know the gain in the system since by definition the NEP is the smallest signal that is equivalent to the rms noise level measured over a 1 Hz bandwidth [i.e., a signal-to-noise (S/N) ratio of 1]. We therefore measured the NEP of several pixels by recording the detector signal as a function of time while modulating the power from the submillimeter illuminator. The NEP was then obtained by Fourier transforming the resulting data and comparing the magnitude of the response to the illuminator modulation (at 2 Hz) with the noise floor nearby to determine the S/N ratio. Fourier transformed real-time output data for one pixel with the source on and off are shown in Fig. 9.

The illuminator was calibrated in a separate experiment²⁰ to determine the temperature as a function of the heater current. In addition, the spectral response curves for all the filters were measured and used to determine the illuminator power radiated in the submillimeter band to the pixels. Dividing this incident power by the S/N ratio gives a direct value for the NEP.

Measurements were made for various values of illuminator power and detector bias. The resulting NEP values for each pixel were under $2.5 \times 10^{-17} \text{ W Hz}^{-1/2}$ for a range of

bias values, and thus within the specification of $7 \times 10^{-17} \text{ W Hz}^{-1/2}$. These measurements were carried out while multiplexing a single column of the array; operating multiple columns simultaneously should have no effect on these values as each column is multiplexed independently.

It should be noted that the true NEP of the detectors should be lower than measured, since the heater illuminator contributes shot noise which will not be present when using the pixel heaters. Nevertheless, the results are within the specification for SCUBA-2, demonstrating that improvements to the prototype to reduce noise will not be necessary.

V. DISCUSSION

Measurements on the prototype 850 μm SCUBA-2 subarray have been extremely successful. The testbed system has operated smoothly. Tests on the array show that it has good uniformity, with no anomalous pixels on the detector wafer in the areas examined. Operation was stable and reproducible from day to day. In particular, these results validate the concept of operating TES detectors with an in-plane multiplexer, as well as this implementation. Noise measurements on several pixels show that the requirements for SCUBA-2 have been met. The success of these measurements has enabled the start of construction of the science grade arrays that will make up the SCUBA-2 instrument.

ACKNOWLEDGMENTS

The SCUBA-2 project is funded by the UK Particle Physics and Astronomy Research Council (PPARC), the JCMT Development Fund, and the Canadian Foundation for Innovation (CFI).

- ¹W. S. Holland *et al.*, *Mon. Not. R. Astron. Soc.* **303**, 659 (1999).
- ²D. Gostick, D. Montgomery, B. Wall, H. McGregor, M. Cliffe, A. Woodcraft, and F. Gannaway, *Proc. SPIE* **5492**, 1743 (2004).
- ³A. L. Woodcraft, F. C. Gannaway, and D. C. Gostick, *Proc. SPIE* **5498**, 446 (2004).
- ⁴M. J. Griffin, *Nucl. Instrum. Methods Phys. Res. A* **444**, 397 (2000).
- ⁵S. F. Lee, J. M. Gildemeister, W. Holmes, A. T. Lee, and P. L. Richards, *Appl. Opt.* **37**, 3391 (1998).
- ⁶F. Simoens *et al.*, *Proc. SPIE* **5498**, 177 (2004).
- ⁷W. D. Duncan *et al.*, *Proc. SPIE* **4855**, 19 (2003).
- ⁸K. D. Irwin *et al.*, *Nucl. Instrum. Methods Phys. Res. A* **520**, 544 (2004).
- ⁹M. D. Audley *et al.*, *Nucl. Instrum. Methods Phys. Res. A* **520**, 479 (2004).
- ¹⁰M. D. Audley *et al.*, *Proc. SPIE* **5498**, 63 (2004).
- ¹¹A. J. Walton *et al.*, *IEE Proc.: Sci., Meas. Technol.* **151**, 110 (2004).
- ¹²W. Parkes, A. M. Gundlach, C. C. Dunare, J. G. Terry, J. T. M. Stevenson, A. J. Walton, and E. Schulte, *Proc. SPIE* **5498**, 407 (2004).
- ¹³P. A. J. de Korte *et al.*, *Rev. Sci. Instrum.* **74**, 3807 (2003).
- ¹⁴C. D. Reintsema *et al.*, *Rev. Sci. Instrum.* **74**, 4500 (2003).
- ¹⁵O. V. Lounasmaa, *Experimental Principles and Methods Below 1 K* (Academic, London, 1974).
- ¹⁶W. Duncan *et al.*, *Nucl. Instrum. Methods Phys. Res. A* **520**, 427 (2004).
- ¹⁷R. P. Welty and J. M. Martinis, *IEEE Trans. Appl. Supercond.* **3**, 2605 (1993).
- ¹⁸Leiden Cryogenics BV, Galgewater No. 21, 2311 VZ Leiden, The Netherlands.
- ¹⁹Haller-Beeman Associates, Inc., 5020 Santa Rita Rd., El Sobrante, CA 94803.
- ²⁰G. Pisano, P. Hargrave, M. Griffin, P. Collins, J. Beeman, and R. Hermoso, *Appl. Opt.* **44**, 3208 (2005).
- ²¹Metglas Inc., 440 Allied Drive, Conway, SC 29526.
- ²²P. L. Richards, *J. Appl. Phys.* **76**, 1 (1994).